

Comparison of ${}^6\text{Li}$ - and ${}^7\text{Li}$ -induced fusion cross sections on ${}^{16}\text{O}$

J. F. Mateja

Physics Department, Tennessee Technological University, Cookeville, Tennessee 38505

A. D. Frawley, L. C. Dennis, and K. Sartor

Physics Department, Florida State University, Tallahassee, Florida 32306

(Received 21 January 1986)

The heavy residues emitted following the interaction of ${}^6\text{Li}$ and ${}^{16}\text{O}$ have been measured for ${}^6\text{Li}$ bombarding energies from 12 to 35 MeV. The gross characteristics of the residue spectra are in qualitative agreement with a fusion-evaporation mechanism. Beginning at Coulomb barrier energies, it is found that the total fusion cross section diverges from the total reaction cross section obtained from optical model fits to ${}^6\text{Li} + {}^{16}\text{O}$ elastic scattering data. The importance of the process which limits the ${}^6\text{Li} + {}^{16}\text{O}$ fusion cross section is attested to by the fact that only 60% of the total reaction strength can be accounted for by fusion at our highest bombarding energies. A comparison of the total fusion cross sections as a function of center-of-mass energy for the ${}^6\text{Li} + {}^{16}\text{O}$ and ${}^7\text{Li} + {}^{16}\text{O}$ entrance channels reveals essentially identical total fusion cross section excitation functions. This result contrasts sharply with the results obtained in an earlier study of ${}^{6,7}\text{Li}$ -induced reactions on ${}^{12,13}\text{C}$ nuclei. In the earlier study, fusion cross sections which were projectile dependent and target independent were observed. Finally, the critical angular momenta have been extracted from the ${}^6\text{Li} + {}^{16}\text{O}$ total fusion cross sections. When compared with the critical angular momenta obtained from an earlier study of the ${}^{10}\text{B} + {}^{12}\text{C}$ entrance channel, a common limitation is found with increasing ${}^{22}\text{Na}$ excitation energy. This result is in sharp contrast with the result of an earlier study of entrance channels which form the ${}^{23}\text{Na}$ compound nucleus, a compound system only one neutron removed from ${}^{22}\text{Na}$.

I. INTRODUCTION

Fusion cross sections in light heavy-ion systems have evoked considerable interest over the past decade. One of the more intriguing findings is the observation of a strong dependence of the maximum fusion cross section on entrance channel.^{1,2} A recent study of fusion cross sections for ${}^6\text{Li}$ - and ${}^7\text{Li}$ -induced reactions on ${}^{12}\text{C}$ and ${}^{13}\text{C}$ targets by Dennis *et al.*³ revealed somewhat unexpected results. The fusion cross section measurements for ${}^6\text{Li} + {}^{12}\text{C}$, ${}^6\text{Li} + {}^{13}\text{C}$, ${}^7\text{Li} + {}^{12}\text{C}$, and ${}^7\text{Li} + {}^{13}\text{C}$ show that the energy dependence of the fusion cross sections and the maximum fusion cross sections depend strongly on the projectile, but not on the target nucleus. The ${}^7\text{Li}$ -induced fusion reactions on both ${}^{12}\text{C}$ and ${}^{13}\text{C}$ targets exhibited maximum fusion cross sections of 950 mb (absolute errors of 110 mb, relative errors of 47 mb), whereas the ${}^6\text{Li}$ -induced fusion cross sections on these target nuclei were only 775 mb (absolute errors of 90 mb, relative errors of 42 mb). In addition, the shapes of the two ${}^7\text{Li}$ -induced fusion excitation functions were essentially identical, and this was also true for the two ${}^6\text{Li}$ -induced fusion excitation functions.

The present study was intended to allow a comparison of the fusion cross sections for ${}^6\text{Li}$ - and ${}^7\text{Li}$ -induced reactions on ${}^{16}\text{O}$, to determine whether or not the systematic behavior described above persists. As the fusion cross sections for the ${}^7\text{Li} + {}^{16}\text{O}$ entrance channel have already been measured,⁴ it was necessary only to measure those for the ${}^6\text{Li} + {}^{16}\text{O}$ entrance channel.

Furthermore, a comparison can be made between the

${}^6\text{Li} + {}^{16}\text{O}$ data and data from another entrance channel, ${}^{10}\text{B} + {}^{12}\text{C}$, which forms the same compound nucleus, ${}^{22}\text{Na}$.⁵ Such comparisons may be useful in attempting to determine the mechanism by which fusion cross sections are limited in light heavy-ion systems.

II. EXPERIMENTAL PROCEDURE

The ${}^6\text{Li}$ beam was provided by the Florida State University super FN tandem Van de Graaff accelerator over a laboratory energy range from 12 to 35 MeV. Self-supporting targets of SiO_2 ($\sim 186 \mu\text{g}/\text{cm}^2$) were employed.

The residues, $A \geq 6$, were mass identified by measuring flight times along a 2.7 m flight path. A microchannel plate start detector marked the initial passage of the heavy residues and a 450 mm² silicon surface barrier detector was used to obtain the stop time and energy of each particle.

A typical two-dimensional mass versus energy spectrum is shown in Fig. 1. As can be seen in this figure, the silicon in the target presented no identification problems since the heavy residues resulting from the decay of the ${}^6\text{Li} + \text{Si}$ compound system were well separated from the residues arising from the ${}^6\text{Li} + {}^{16}\text{O}$ decays.

Angular distributions of the evaporation residues were measured from 5° to 65° in the laboratory to obtain the total residue yield. Monitors, positioned to the left and right of the beam, were used to normalize between runs.

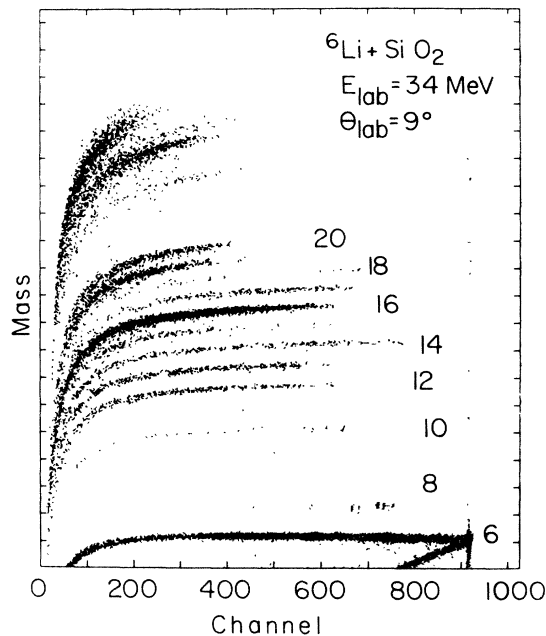


FIG. 1. A representative mass versus energy contour map for the ${}^6\text{Li} + {}^{16}\text{O}$ entrance channel.

Since the shapes of the residue angular distributions change slowly as a function of energy (see Fig. 2), complete angular distributions were only measured at energies of 12, 18, 24, 30, and 34 MeV. The total cross sections at other energies were obtained by measuring the residues at a single angle, $\theta_{\text{lab}} = 9^\circ$, and using the ratio of the single-

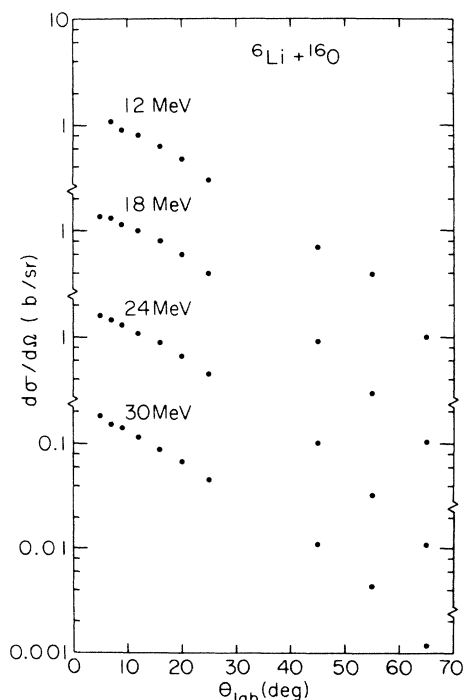


FIG. 2. Angular distribution of the evaporation residues summed over all residue masses for the ${}^6\text{Li} + {}^{16}\text{O}$ entrance channel.

angle yield to the angle-integrated yield obtained by interpolating smoothly between the energies at which angular distributions were measured.

The absolute cross sections were determined by measuring the product of the target thickness and detector solid angles. For this measurement, 15 MeV ${}^{12}\text{C}$ ions were elastically scattered from the SiO_2 target. At angles from 18° to 21° where the elastic scattering peaks from Si and O were well separated, the ${}^{12}\text{C} + {}^{16}\text{O}$ scattering was found to be Rutherford. The magnitudes of the elastic scattering cross sections were found to be in good agreement with optical model curves obtained using the parameters of Poling *et al.*⁶ The estimated uncertainty in the absolute cross sections is 10%.

The same target was used for both the ${}^6\text{Li} + {}^{16}\text{O}$ and ${}^7\text{Li} + {}^{16}\text{O}$ measurements. The relative total cross section normalization for the two reactions was obtained by measuring both the ${}^6\text{Li} + {}^{16}\text{O}$ and ${}^7\text{Li} + {}^{16}\text{O}$ angular distributions at 34 MeV without moving the target between runs. Therefore, we believe that the uncertainty in the relative cross sections at 34 MeV is considerably smaller than the uncertainty in the absolute cross section measurements. The resulting relative uncertainty between the ${}^6\text{Li} + {}^{16}\text{O}$ and ${}^7\text{Li} + {}^{16}\text{O}$ residue cross sections at any energy is judged to be only about 5%. This uncertainty arises from counting statistics, extrapolation of the residue angular distributions to 0° and beyond 65° , and normalization of the single-angle excitation functions to the complete angular distributions. The two angular distributions measured at 34 MeV are shown in Fig. 3.

In evaluating the total fusion cross section for the ${}^6\text{Li} + {}^{16}\text{O}$ entrance channel, the energy spectra of all mass groups were inspected for evidence of nonfusion events (i.e., direct transfer, inelastic scattering, and knockout) before that mass group was included in the calculation of the total fusion cross section. Events which formed discrete peaks in the energy spectrum of a particular exit channel were considered to be nonfusion and were excluded.

Using the above criteria, no significant evidence of nonfusion events was found for residue mass groups from 8

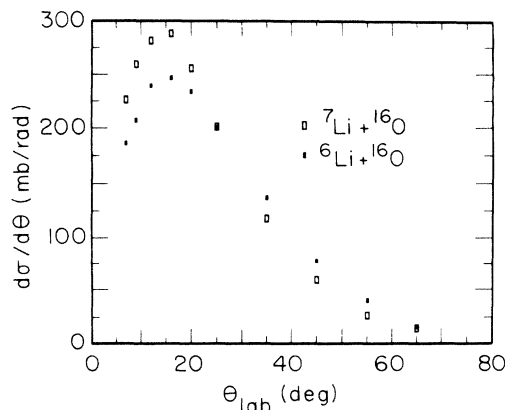


FIG. 3. A comparison of the ${}^6\text{Li} + {}^{16}\text{O}$ and ${}^7\text{Li} + {}^{16}\text{O}$ angular distributions at ${}^6\text{Li}$ and ${}^7\text{Li}$ laboratory bombarding energies of 34 MeV.

to 21 in the ${}^6\text{Li} + {}^{16}\text{O}$ investigation. Discrete peaks at near-projectile velocities were, however, found in the mass 7 energy spectrum (see Fig. 1). This yield, whose integrated strength varied from 1 to 4 mb depending upon energy, was not included in the calculation of the total fusion cross section. The total fusion yield, therefore, was taken to be the sum of the yields for masses 8 through 21.

The total fusion cross section for the ${}^7\text{Li} + {}^{16}\text{O}$ system, to be compared with the ${}^6\text{Li} + {}^{16}\text{O}$ results later in this paper, were taken from Ref. 4. In this earlier work, criteria similar to that outlined above were used. It should also be noted that in the Ref. 4 investigation the heavy residue spectra for the ${}^7\text{Li} + {}^{16}\text{O}$ system were compared with the heavy residue spectra from three other entrance channels which formed the ${}^{23}\text{Na}$ compound nucleus. When the energy spectra for the four entrance channels were compared, any nonfusion yield present in the ${}^7\text{Li} + {}^{16}\text{O}$ data should have been readily apparent as it is unlikely, for example, that direct transfer would appear in the same residue for all four entrance channels. No evidence of non-fusion yield in masses 8 through 22 was found in the ${}^7\text{Li} + {}^{16}\text{O}$ investigation. In Ref. 4, the total ${}^7\text{Li} + {}^{16}\text{O}$ fusion cross section was found by summing the yield in mass groups 8 through 22.

Finally, the efficiency of the time-of-flight system for any particle can vary with the particle's charge, mass, and energy. The efficiency varies with these residue attributes due to the different number of electrons produced in the channel-plate start detector. High-energy, low-mass ions, for example, produce few electrons which result in a small signal from the channel-plate detector. Some of these signals can be so small that they fall below the threshold necessary to trigger the timing circuit, leading to a loss of events in the time versus energy spectrum. The efficiency was checked experimentally by comparing the elastic yield in the singles energy spectrum with the corresponding elastic yield in the time spectrum. In addition to the ${}^6\text{Li}$ and ${}^7\text{Li}$ beams used in the fusion measurements, a ${}^{12}\text{C}$ beam was used to check the efficiency for mass 12. Corrections on the order of 40% were required for ${}^6\text{Li}$ while for the mass 12 group the system was found to be 100% efficient. As we have not measured the efficiency for each mass group, we have assumed that the efficiency changes smoothly between masses and have interpolated to compute the correction for each mass. While the correction to an individual mass in the mass 6 to 11 group is large, the effect on the total cross section is negligible due to the fact that these masses account for a very small fraction ($\sim 4\%$) of the total fusion strength.

III. EXPERIMENTAL RESULTS AND DISCUSSION

A. Individual residue cross sections

Excitation functions for the individual evaporation residues for ${}^6\text{Li} + {}^{16}\text{O}$ are presented in Fig. 4. In grouping the different residue masses in this figure, it has been assumed that the only light particles emitted in the decay of the ${}^{22}\text{Na}$ compound nucleus are protons, neutrons, and alpha particles. Experimental studies in this mass and ener-

gy region indicate that d, t, and ${}^3\text{He}$ decays, which might be expected to compete, are weak.^{3,7}

The behavior of these excitation functions appears to be in qualitative agreement with a fusion-evaporation process. The decay channels available to the ${}^{22}\text{Na}$ compound nucleus and the capture Q value for the ${}^6\text{Li} + {}^{16}\text{O}$ to form the compound system are presented in Fig. 5. As can be seen in this figure, there are different energy thresholds below which a particular number of light particles cannot be emitted (these thresholds correspond to the energies required to form the ground states of the relevant heavy residues). When the energy threshold for the emission of a particular number of light particles has been exceeded, the cross section to the residues in that group would be expected to increase rapidly as the level density in each residue begins to increase. In addition, one would expect the mass groups corresponding to one, two, three, four, and five light-particle emissions to peak at successively higher energies, each group reaching a maximum near the energy at which the next highest group begins to show a significant yield. The experimental excitation functions shown in Fig. 4 exhibit the expected characteristics at the

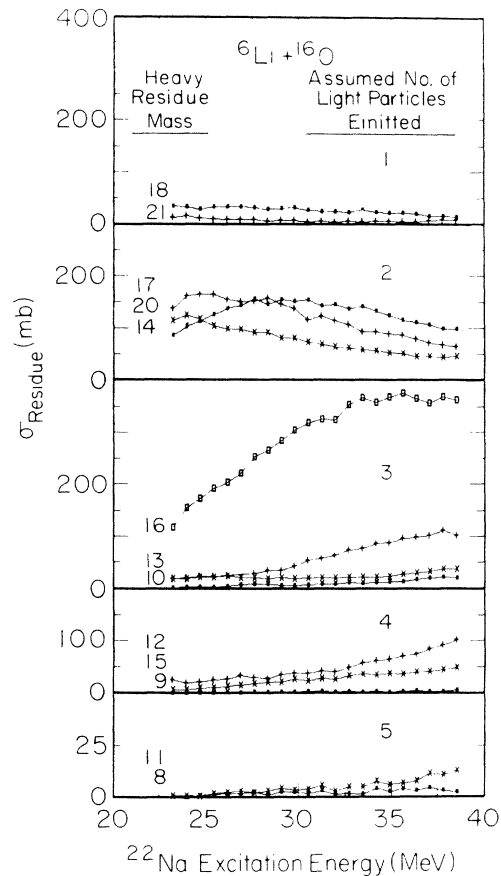


FIG. 4. Excitation functions of the heavy residue produced in the ${}^6\text{Li} + {}^{16}\text{O}$ experiment. The lines are drawn only to help guide the eye. For the strong residue masses, the relative uncertainties due to counting statistics are approximately twice the size of the data points. For the weak residue masses, the relative uncertainties are approximately four times the data point size.

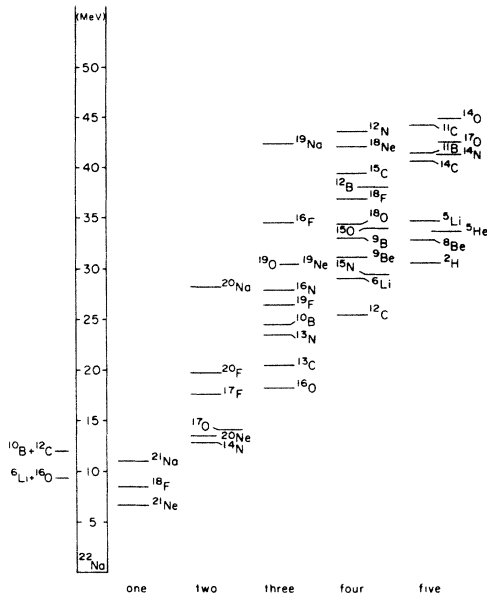


FIG. 5. Ground states of the residual nuclei available for the decay of ^{22}Na . The residual nuclei have been grouped according to the number of light particles which must be emitted to reach a particular decay channel (assuming that the light particle emission involves only protons, neutrons, and α particles).

appropriate energies. Similar results have been found for other systems in this mass and energy region.⁸

B. Limitation in the $^6\text{Li} + ^{16}\text{O}$ total fusion cross section

The total fusion and total reaction cross sections for the $^6\text{Li} + ^{16}\text{O}$ entrance channel are displayed in Fig. 6. The total reaction cross section was determined from optical model parameters reported for this system by Poling *et al.*⁶ As the optical model parameter set used was obtained by simultaneously fitting elastic scattering angular distributions which spanned the energy range currently being studied ($E_{\text{lab}} = 4.5$ to 50.6 MeV), it is expected that the energy dependence of the total reaction cross section is correctly predicted.

As with many other systems in this mass and energy region,^{3,4,8,9} the fusion cross section is significantly smaller than the total reaction cross section, even at low bombarding energies. Two limitation mechanisms have been proposed. In the first, the limitation in the fusion cross section is attributed to having reached a critical density of states in the compound nucleus.¹⁰ The principal signature of such a limitation would be that the critical angular momentum lines for different entrance channels which form the same compound system converge as the energy is increased. The critical angular momentum may be extracted from the total fusion cross section according to the sharp-cutoff approximation

$$\sigma_{\text{fus}} = \pi \lambda^2 \sum_{l=0}^{l_{\text{cr}}} (2l+1).$$

The critical angular momenta obtained in this way from

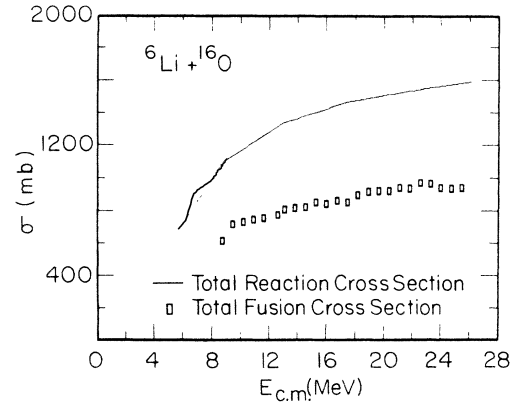


FIG. 6. A comparison of the total fusion and total reaction cross sections for the $^6\text{Li} + ^{16}\text{O}$ entrance channel.

our $^6\text{Li} + ^{16}\text{O}$ data are shown as a function of ^{22}Na excitation energy in Fig. 7. Also shown in this figure is the grazing angular momentum curve for this entrance channel. The grazing angular momenta were obtained from an optical model parametrization of $^6\text{Li} + ^{16}\text{O}$ elastic scattering by Poling *et al.*⁶ The large difference in the grazing and critical angular momenta curves is again an indication that there is a significant limitation occurring in the fusion channel for the $^6\text{Li} + ^{16}\text{O}$ scattering process.

Also shown in Fig. 7 are the critical angular momenta for the $^{10}\text{B} + ^{12}\text{C}$ entrance channel, an entrance channel which also forms the ^{22}Na compound nucleus.⁵ As can be seen, the two entrance channels are limited by a common value of l_{crit} at each ^{22}Na excitation energy. Such a result has been taken as a signature that a critical density of compound nuclear states with the appropriate spin has been reached.¹⁰⁻¹²

While such a limitation in l_{crit} could be produced by a

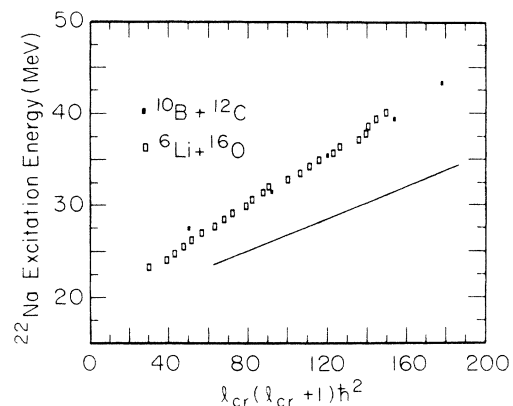


FIG. 7. A comparison of the critical angular momenta for two entrance channels, $^6\text{Li} + ^{16}\text{O}$ and $^{10}\text{B} + ^{12}\text{C}$, used to form the ^{22}Na compound nucleus. The fusion cross sections used to compute the $^{10}\text{B} + ^{12}\text{C}$ critical angular momenta were taken from Ref. 5. The solid line represents the grazing angular momenta for the $^6\text{Li} + ^{16}\text{O}$ entrance channel. The grazing angular momenta were obtained from an optical model parametrization using the optical model parameters from Ref. 6.

critical density of compound nuclear states, the fact that two entrance channels's critical angular momenta approach a common limit does not necessarily mean that the limitation was produced by such a mechanism. Studies involving the ${}^{23}\text{Na}$ compound nucleus are a case in point. The four entrance channels which form the ${}^{23}\text{Na}$ compound nucleus (${}^{11}\text{B} + {}^{12}\text{C}$, ${}^7\text{Li} + {}^{16}\text{O}$, ${}^9\text{Be} + {}^{14}\text{N}$, and ${}^{10}\text{B} + {}^{13}\text{C}$), have been investigated over an energy range similar to that in the present work (~ 1 to 3 times the energy of the Coulomb barrier).^{4,8,13,14} In these studies, three of the four entrance channels were found to approach a common limitation in a plot of l_{crit} vs ${}^{23}\text{Na}$ excitation energy. The fourth, ${}^{11}\text{B} + {}^{12}\text{C}$, clearly did not. As the ${}^{11}\text{B} + {}^{12}\text{C}$ entrance channel brings in the largest angular momentum at a given compound nuclear excitation energy, this channel should have been the first and the most severely limited if the limitation was due to having reached a critical density of compound nuclear states. As the other three entrance channels bring in less angular momentum than the ${}^{11}\text{B} + {}^{12}\text{C}$ at a given ${}^{23}\text{Na}$ excitation energy, a mechanism based upon having reached a critical density of states is clearly ruled out for these entrance channels. Without the ${}^{11}\text{B} + {}^{12}\text{C}$ data, however, an erroneous conclusion could easily have been drawn. Other mechanisms which could limit these fusion cross sections will be discussed below.

A result similar to that for the ${}^{23}\text{Na}$ compound nucleus has been found in a subsequent study of the ${}^{19}\text{F}$ compound system with the ${}^6\text{Li} + {}^{13}\text{C}$ and ${}^7\text{Li} + {}^{12}\text{C}$ entrance channels.³ In this work, no evidence of a compound-nucleus-type limitation was observed over an energy range from 1 to 3 times the Coulomb barrier energy, even though a strong fusion cross section limitation was evident in this energy region. In yet another study, the Oak Ridge group¹⁵ has recently examined the ${}^{12}\text{C} + {}^{14}\text{N}$ and ${}^{10}\text{B} + {}^{16}\text{O}$ entrance channels. They find in this energy region that while the limiting angular momenta for these reactions appear to reach a common limit, a more careful inspection reveals that the critical angular momentum lines actually have different slopes in the region where there is supposed to be a common limitation. Such a result is not consistent with a compound nucleus induced limit to fusion. From the above results, it is no longer clear that a common limitation in l_{crit} is necessarily a signature of a fusion cross section limitation imposed by a critical density of compound nuclear states. Such a limitation may simply be a consequence of entrance channel Q value, moment of inertia, and competing reaction processes which, quite by accident, combine to bring the critical angular momenta for these systems to what appears to be a common limit.

For the ${}^{11}\text{B} + {}^{12}\text{C}$ and ${}^{10}\text{B} + {}^{13}\text{C}$ entrance channels a study of the light particles emitted in these reactions suggests that the limitation could be brought about by a competing reaction process, projectile breakup.¹⁶ In the study of the ${}^{10}\text{B} + {}^{16}\text{O}$ and ${}^{12}\text{C} + {}^{14}\text{N}$ entrance channels by Gomez del Campo *et al.*,¹⁵ a different reaction mechanism was found to compete strongly with fusion for entrance channel flux. In these cases the dominant competing reaction appears to be direct transfer. While the process responsible for fusion cross section limitations ap-

pears to be competition with other reaction mechanisms, identifying the major competing channels requires further experimental investigation.

C. Comparison of the ${}^6\text{Li} + {}^{16}\text{O}$ and ${}^7\text{Li} + {}^{16}\text{O}$ fusion cross sections

The excitation functions for the total fusion cross sections for the ${}^6\text{Li} + {}^{16}\text{O}$ and ${}^7\text{Li} + {}^{16}\text{O}$ entrance channels as a function of center-of-mass energy are displayed in Fig. 8. For comparison purposes, the relative errors, as opposed to the absolute errors, are shown.

In the earlier study of ${}^{6,7}\text{Li}$ projectiles on ${}^{12,13}\text{C}$ targets, the strengths of the fusion cross sections were found to be independent of target but strongly dependent upon projectile.³ In the $\text{Li} + \text{C}$ study, the fusion excitation functions for ${}^6\text{Li}$ on ${}^{12}\text{C}$ and ${}^{13}\text{C}$ targets were essentially identical and exhibited maximum fusion strengths of 775 mb. The excitation functions for ${}^7\text{Li}$ -induced fusion cross sections, again on ${}^{12}\text{C}$ and ${}^{13}\text{C}$ targets, were similar in shape to one another with maximum cross sections of 950 mb. As can be seen in Fig. 8, quite different results are obtained for ${}^6\text{Li}$ - and ${}^7\text{Li}$ -induced reaction on ${}^{16}\text{O}$. Here, one finds similarly shaped fusion excitation functions with similar maximum cross sections for both projectiles.

The present result shows that the process involved is more complicated than one might have concluded from the earlier $\text{Li} + \text{C}$ work of Dennis *et al.*³ When considered in context with this earlier experiment, the present result, no observed difference in maximum fusion cross section from one projectile to the other, shows that the target does play an important role in determining the total fusion strength.

We believe that the above experimental results simply point to the fact that the problem is multifaceted and that no one single reaction feature is responsible for the fusion cross section energy dependence or for the magnitude of the maximum fusion cross section.

IV. SUMMARY

Evaporation residues resulting from the interaction of ${}^6\text{Li}$ and ${}^{16}\text{O}$ have been mass identified with a time-of-

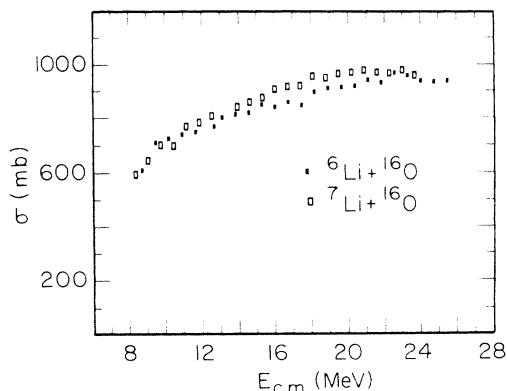


FIG. 8. Total fusion cross sections versus center-of-mass energy for the ${}^6\text{Li} + {}^{16}\text{O}$ and ${}^7\text{Li} + {}^{16}\text{O}$ entrance channels.

flight system. Little evidence for nonfusion events was present in any of the residue energy spectra. In addition, if one assumes that p, n, and α -particle emission dominate the decay process, the energy dependence of these residues is found to be in qualitative agreement with what one would expect from a fusion-evaporation mechanism.

A comparison of the ${}^6\text{Li} + {}^{16}\text{O}$ and ${}^7\text{Li} + {}^{16}\text{O}$ fusion cross section excitation functions reveals that both the shapes and magnitudes of the cross sections are similar. In contrast, earlier measurements of the fusion cross sections for ${}^6\text{Li}$ - and ${}^7\text{Li}$ -induced reactions on ${}^{12}\text{C}$ and ${}^{13}\text{C}$ targets found a substantial fusion cross section difference which appeared to be solely projectile dependent. The fact that one observes fusion cross sections which vary with lithium isotope in one case (the Li + C results) but not in another case where the same lithium isotopes are used (the Li + O results), illustrates the importance of both partners in these reaction processes.

Finally, the critical angular momenta extracted from the ${}^6\text{Li} + {}^{16}\text{O}$ data have been compared as a function of ${}^{22}\text{Na}$ excitation energy with the critical angular momenta for the ${}^{10}\text{B} + {}^{12}\text{C}$ entrance channel. The two entrance

channels yield similar values of l_{crit} at each compound nucleus excitation energy studied. This result is particularly surprising in view of the fact that over a similar energy region the ${}^7\text{Li} + {}^{16}\text{O}$ and ${}^{11}\text{B} + {}^{12}\text{C}$ entrance channels, systems which form a compound nucleus only one neutron removed from the ${}^{22}\text{Na}$ compound nucleus studied in the present experiment, show no sign of such a common limitation. Such results, we believe, call into question earlier assumptions that the observation of a common limitation in the critical angular momentum was a signature that one had reached a critical density of states in the compound nucleus.

ACKNOWLEDGMENTS

The authors would like to thank Tennessee Tech students Aaron Manka, Gregory Gentry, and Dale Baltimore for their assistance in the collection and analysis of this data. This research was supported in part by the U.S. Department of Energy under Contract No. DE-AS05-80ER10714 and by the National Science Foundation.

-
- ¹D. G. Kovar, D. F. Geesaman, T. H. Braid, Y. Eisen, W. Henning, T. R. Ophel, M. Paul, K. E. Rehm, S. J. Sanders, P. Sperr, J. P. Schiffer, S. L. Tabor, S. Vigdor, B. Zeidman, and F. W. Prosser, Jr., *Phys. Rev. C* **20**, 1305 (1979).
- ²J. Gomez del Campo, R. G. Stokstad, J. A. Biggerstaff, R. A. Dayras, A. H. Snell, and P. H. Stelson, *Phys. Rev. C* **19**, 2170 (1979).
- ³L. C. Dennis, K. M. Abdo, A. D. Frawley, and K. W. Kemper, *Phys. Rev. C* **26**, 981 (1982).
- ⁴J. F. Mateja, J. Garman, D. E. Fields, R. L. Kozub, A. D. Frawley, and L. C. Dennis, *Phys. Rev. C* **30**, 134 (1984).
- ⁵J. S. Hanspal, L. C. Dennis, A. D. Frawley, R. A. Parker, K. Sartor, and S. J. Padalino (unpublished).
- ⁶J. E. Poling, E. Norbeck, and R. R. Carlson, *Phys. Rev. C* **13**, 648 (1976).
- ⁷A. C. Xenoulis, A. E. Aravatinos, C. J. Lister, J. W. Olness, and R. L. Kozub, *Phys. Lett.* **106B**, 461 (1981).
- ⁸J. F. Mateja, A. D. Frawley, L. C. Dennis, K. Abdo, and K. W. Kemper, *Phys. Rev. C* **25**, 2963 (1982).
- ⁹J. S. Eck, J. R. Leigh, T. R. Ophel, and P. D. Clark, *Phys. Rev. C* **21**, 2352 (1980).
- ¹⁰S. M. Lee, T. Matsuse, and A. Arima, *Phys. Rev. Lett.* **45**, 165 (1980).
- ¹¹J. P. Wieleczko, S. Harar, M. Comjeaud, and F. Saint-Laurent, *Phys. Lett.* **93B**, 35 (1980).
- ¹²F. Saint-Laurent, M. Comjeaud, and S. Harar, *Nucl. Phys.* **A327**, 517 (1979).
- ¹³J. F. Mateja, A. D. Frawley, L. C. Dennis, K. Abdo, and K. W. Kemper, *Phys. Rev. Lett.* **47**, 311 (1981).
- ¹⁴J. F. Mateja, A. D. Frawley, R. A. Parker, and K. Sartor, *Phys. Rev. C* **33**, 1307 (1986).
- ¹⁵J. Gomez del Campo, J. A. Biggerstaff, R. A. Dayras, D. Shapira, A. H. Snell, P. H. Stelson, and R. G. Stokstad, *Phys. Rev. C* **29**, 1722 (1984).
- ¹⁶J. F. Mateja, J. Garman, and A. D. Frawley, *Phys. Rev. C* **28**, 1579 (1983).